

DMD #63305

## SHORT COMMUNICATION

### **Suppression of Pulmonary CYP2A13 Expression by Carcinogen-induced Lung**

### **Tumorigenesis in a CYP2A13-humanized Mouse Model**

Zhihua Liu, Vandana Megaraj, Lei Li, Stewart Sell, Jing Hu, and Xinxin Ding

*Wadsworth Center, New York State Department of Health, and School of Public Health,  
University at Albany, Albany, NY 12201 (ZL, VM, SS, JH, XD); College of Nanoscale Science  
and Engineering, SUNY Polytechnic Institute, Albany, NY 12203 (LL, XD)*

DMD #63305

**RUNNING TITLE:** *Suppression of CYP2A13 expression by lung tumorigenesis*

**ADDRESS CORRESPONDENCE TO:**

Dr. Xinxin Ding, College of Nanoscale Science and Engineering, SUNY Polytechnic Institute,  
257 Fuller Road, NanoFab East, Albany, NY 12203; Tel. 518-956-7057; E-mail:

[xding@sunycnse.com](mailto:xding@sunycnse.com)

Number of Text Pages: 14

Number of Figures: 2

Number of References: 24

Number of words:

Abstract: 244

Introduction: 526

Discussion: 595

**ABBREVIATIONS:** P450, cytochrome P450; NNK, 4-(methylnitrosamino)-1-(3-pyridyl)-1-butanone; SAP, serum amyloid P component; GAPDH, glyceraldehyde 3-phosphate dehydrogenase

## ABSTRACT

CYP2A13 is a human cytochrome P450 (P450) enzyme important in the bioactivation of the tobacco-specific lung procarcinogen 4-(methylnitrosamino)-1-(3-pyridyl)-1-butanone (NNK). CYP2A13 expression levels vary dramatically among lung biopsy samples from patients, presumably due in part to a suppression of CYP2A13 expression by disease-associated inflammation. Here, we have determined whether CYP2A13 expression in the lungs of CYP2A13-humanized mice is suppressed by the presence of lung tumors. Tissues from an NNK lung-tumor bioassay were examined. CYP2A13-humanized mice (95-100%) had multiple lung tumors at 16 weeks after NNK (30 or 50 mg/kg) treatment; whereas only ~9% of saline-treated CYP2A13-humanized mice had lung tumor (~1/lung). Mice with lung tumors, from the NNK-treated groups, were used for dissecting adjacent tumor-free lung tissues; whereas mice without visible lung tumors, from the saline-treated group, were used as controls. Compared to the controls, the levels of CYP2A13 protein and mRNA were both reduced significantly (by  $\geq 50\%$ ) in the NNK-treated groups. The levels of mouse CYP2B10 and CYP2F2 mRNAs were also significantly lower in the dissected normal lung tissues from tumor-bearing mice, than in lungs from the control mice. Pulmonary tissue levels of three proinflammatory cytokines, TNF- $\alpha$ , IFN- $\gamma$ , and IL-6, were significantly higher in the tumor-bearing mice than in the controls, indicating occurrence of low-grade lung inflammation at the time of necropsy. Taken together, these findings support the hypothesis that CYP2A13 levels in human lungs can be suppressed by disease-associated inflammation in tissue donors, a scenario causing underestimation of CYP2A13 levels in healthy lungs.

## Introduction

CYP2A13, a functional member of the human *CYP2A* gene subfamily, is selectively expressed in the respiratory tract (Koskela et al., 1999; Su et al., 2000; Zhu et al., 2006), and is the most efficient P450 enzyme in the metabolic activation of the tobacco-specific lung procarcinogen 4-(methylnitrosamino)-1-(3-pyridyl)-1-butanone (NNK) (Su et al., 2000; He et al., 2004; Jalas et al., 2005). CYP2A13 protein has been detected in human nasal mucosa and lung (Wong et al., 2005; Zhang et al., 2007). In human lungs, levels of CYP2A13 protein expression were correlated with rates of lung microsomal NNK metabolic activation (Zhang et al., 2007). The *CYP2A13*\*2 allele, which has a decreased level of gene expression, and encodes a variant CYP2A13 protein with reduced activity toward NNK (Zhang et al., 2002; D'Agostino et al., 2008), is associated with a reduced risk of smoking-induced lung adenocarcinoma (Wang et al., 2003). More recently, CYP2A13 was found to mediate NNK-induced lung tumorigenesis in a CYP2A13-humanized mouse model (Megaraj et al., 2014). These findings strongly suggest that CYP2A13 plays an important role in the metabolic activation of NNK in the respiratory tract of human smokers.

A large interindividual variation in the detected levels of CYP2A13 expression (<2 to 20 fmol/mg microsomal protein) in human lung biopsy samples was previously reported (Zhang et al., 2007). Given the potential impact of differences in lung CYP2A13 expression levels on the susceptibility to tobacco smoke-induced lung cancer, we have been searching for factors that dictate the apparently large interindividual variations in CYP2A13 expression. While some *CYP2A13* genetic variants (e.g., \*2 and 7520C>G) are associated with decreased allelic expression in human lung (Zhang et al., 2004; D'Agostino et al., 2008; Wu et al., 2009), we also obtained evidence supporting the hypothesis that CYP2A13 levels in human lung can be suppressed by inflammation associated with disease status in tissue donors (Wu et al., 2013). In

DMD #63305

the latter study, we demonstrated that the bacterial endotoxin lipopolysaccharide (LPS) can suppress CYP2A13 expression in vitro, in the NCI-H441 human lung cell line, and in vivo, in a CYP2A13-humanized (CYP2A13-transgenic/*Cyp2a5*-null) mouse model, via a mechanism that involves regulatory sequences in the *CYP2A13* promoter region and the nuclear factor NF- $\kappa$ B.

The human lung biopsy samples examined in our previous study were mainly resected, histologically normal lung tissues from patients with lung tumors (Zhang et al., 2007). The aim of this study was to test the hypothesis that CYP2A13 levels in resected non-tumor lung tissues can be suppressed by the inflammation induced by the presence of lung tumors, in the CYP2A13-humanized mouse model. Lung tumors were induced in CYP2A13-humanized mice (on A/J background) by a single, intraperitoneal NNK injection. Tumor-bearing mice and control (saline-treated, tumor-free) mice were examined 16 weeks later for levels of CYP2A13 expression in lung tissues, and for signs of pulmonary or systemic inflammation. Our results provide further experimental proof to support the idea that the levels of CYP2A13 (and possibly other CYPs) detected in patient-derived lung tissues are lower than the levels present in normal, healthy human lung, a notion that has significant implications for efforts to delineate the roles of human lung P450 enzymes in xenobiotic metabolism, pulmonary pathogenesis, and chemical carcinogenesis.

## Materials and Methods

**Animal treatments.** All procedures involving animals were approved by the Institutional Animal Care and Use Committee of the Wadsworth Center. The conditions and protocols for NNK lung tumor bioassay for the CYP2A13-humanized mouse model (CYP2A13/2B6/2F1-transgenic/*Cyp2a5*-null; A/J-N5) have been described (Megaraj et al., 2014). Tissues from that project were used for this study. For tumor induction, 8-week-old female mice were treated with a single i.p injection of either saline or NNK (either 30 or 50 mg/kg body weight).

**Blood collection, tissue dissection, lung homogenate preparation, and ELISA for cytokine detection.** Post sacrifice, blood was collected from left ventricle and serum was stored at -80 °C until use for cytokine determination. Mouse lungs were dissected on ice to removal all tumors visible from the surface; the remaining tumor-free, adjacent lung tissues were quickly frozen on dry ice and stored at -80 °C until use. In pilot studies, the dissection procedure (<5 min/mouse) was found to not affect CYP2A13 protein or mRNA levels. The frozen lung tissues were weighed, thawed, and placed into tubes containing 1 ml of T-PER on ice (Tissue Protein Extraction Reagent, Thermo, Rockford, IL), containing freshly added Halt protease inhibitor single-use cocktail (100×), and homogenized on ice with a Polytron (PT 10-35, Kinematica). Lung homogenates were centrifuged at 10000 ×g for 5 min at 4 °C; the supernatant was transferred to a new tube and stored at -80 °C until use. IL-6, TNF-α, and IFN- γ were determined in sera and lung homogenates using the mouse cytokine DuoSet ELISA kit (R & D System, Minneapolis, MN). Lung tissue homogenates were prediluted with 1% BSA in PBS to a final concentration of 1 mg lung protein/ml.

**RNA isolation and PCR analysis.** Total RNA was isolated from mouse lung and liver using Trizol reagent (Invitrogen, Carlsbad, CA). First-strand cDNA was prepared using the

DMD #63305

SuperScriptIII first-strand synthesis system (Invitrogen). Briefly, 2.5 µg of total lung RNA or 5 µg of total liver RNA was treated with DNase I (Invitrogen) at room temperature for 15 min, and then were mixed with standard amounts of oligo(dT) and other components of the system in final volume of 20 µl. Each reaction mixture was incubated at 50°C for 50 min. PCR reactions were carried out essentially as described (Zhang et al., 2007). Levels of various mRNAs were normalized to those of glyceraldehyde-3-phosphate dehydrogenase (GAPDH). Primers used were: GAPDH-F (5'-tgtgaacggatttgccgta-3') and GAPDH-R (5'-tcgctcctggaagatggtga-3') (Wei et al., 2012); mSAP-F (5'-tactgctttggatgtttgtcttcac-3') and mSAP-R (5'-tcagcttcacatgatttcag-3') (Charles et al., 2006); CYP2B10-F (5'-caggtgatcggtcacacc-3') and CYP2B10-R (5'-tgactgcactgagatggcatt-3'); CYP3A11-F (5'-ggatgagatcgatgaggctctg-3') and CYP3A11-R (5'-caggtattccatctccatcacagt-3') (Pan et al., 2000); CYP2F2-F1 (5'-aaagaagcatcgaggagc-3') and CYP2F2-R1 (5'-cgaagacgacagagcagat-3') (Braeuning et al., 2009); CYP2A13E6F (5'-acctggtgatgaccaccc-3') and CYP2A13E7R (5'-cgtggatcactgcctctg-3') (Zhang et al., 2004).

**Microsome preparation and immunoblot analysis.** Microsome preparation and immunoblot analysis were performed essentially as described previously (Ding and Coon, 1990). Microsomal proteins were separated on NuPAGE Bis-Tris Mini gels (10%) (Invitrogen). Rabbit antibodies against CYP2A5 (Gu et al., 1998) or calnexin (Genscript, Piscataway, NJ) and a goat anti-rabbit secondary antibody (Sigma) were used.

**Histopathological analysis of dissected adjacent lung tissues.** Frozen lung tissues that have been dissected to remove all visible tumors were thawed in saline at 4°C for 30 min, and then fixed in 4% PFA overnight, and embedded with paraffin. To search for interior tumors that were missed by the initial visual inspection, 10 serial sections covering each entire lung lobe were obtained and stained with H&E for histopathological analysis. The cross-sectional diameters of the adenoma lesions in each slide, measured by a stage micrometer transposed onto

DMD #63305

the photomicrographs of the slides, were used to calculate the area of the lesions. The length and width of the tissue section on the slide was also measured, and used for calculation of the total area. The percent area of the section containing tumor tissue was calculated by adding up the area of the lesions for each section and dividing by the total area of the tissue section  $\times 100$ . The number of cells within tumorous lesions and the total number of cells on each section were also counted.

**Data analysis and statistics.** Quantitative data are expressed as means  $\pm$  S.E. in all groups. For comparison of gene and protein expression in control and tumor-bearing mice, either Student's t-test or one-way ANOVA with Dunnett's post-hoc test was performed, as indicated.



## RESULTS

### **Repression of CYP2A13 expression in the lungs of NNK-treated, tumor-bearing mice**

Four different NNK doses (30, 50, 100, and 200 mg/kg) were used in the original tumor bioassay (Megaraj et al., 2014); but tissues from only the two lower doses and the saline control group are analyzed here, as the lungs from the two high dose groups had too many tumors, which made it difficult to dissect adjacent “tumor-free” tissues. As reported in the original study (Megaraj et al., 2014), essentially all NNK-treated CYP2A13-humanized mice had observable lung tumors at 16 weeks after the NNK treatment (tumor frequency: 100% and 95%; tumor multiplicity: 13.1 and 4.4 tumors per lung; for the 50 mg/kg and 30 mg/kg NNK dose groups, respectively). Approximately 9% of saline-treated CYP2A13-humanized mice also had lung tumor (each mouse had ~1 tumor per lung). Ten mice with lung tumors, from each of the two NNK-treated groups, were used for dissecting adjacent lung tissues; whereas three mice without lung tumors, from the saline treated group, were used as controls. The lung tumors were visible from the surface. The identification of lung tumors was confirmed by histopathological analysis (Megaraj et al., 2014). The boundaries of the tumors, which distort the alveolar architecture, were usually well demarcated, allowing easy removal of the tumors during dissection.

The “tumor-free”, adjacent lung tissues are defined as tissues without visible tumors. In a pilot study, we assessed the potential presence of smaller tumors, which were too small to be seen, by performing histological analysis of dissected lung tissues from four NNK-treated mice (one lung lobe each). By examining serial sections through the entire lung lobes, we found 2-5 additional (small) tumorous lesions per lung lobe, from which visible tumors had been removed. However, these small tumorous lesions were found to correspond to, on average, no more than ~2% (based on space occupied) to ~6% (based on the number of cells) of the lung lobes analyzed (Supplemental Table 1).

DMD #63305

CYP2A13 protein expression was examined by immunoblot analysis in microsomes prepared from tumor-free lung tissues. CYP2A13 protein was detected in both NNK-treated groups and the saline control group (Fig. 1A). As reported recently, the anti-CYP2A5 polyclonal antibody detects a non-specific band in the lungs of both *Cyp2a5*-null mice and the CYP2A13-humanized mice (Wei et al., 2013). As expected, the CYP2A13 band was not detected in lung microsomes from the *Cyp2a5*-null mice, which served as a negative control. Compared to the saline treated group, the level of CYP2A13 protein was reduced significantly (by >60%) in both NNK-treated groups (Fig. 1B).

CYP2A13 mRNA expression was also examined, in total RNA prepared from tumor-free lung tissues. Compared to the saline control group, CYP2A13 mRNA levels were decreased by ~50% in the 30 mg/kg group (though statistical significance was not reached) and by ~80% in the 50 mg/kg group ( $p < 0.01$ ) (Fig. 1C). Notably, there was no difference in CYP2A13 mRNA level between saline and NNK (30 or 50 mg/kg) groups at one week after dosing (Fig. 1D), a result indicating that NNK injection per se did not suppress lung CYP2A13 expression.

The effects of lung tumorigenesis on the expression of mouse P450s were also examined. The levels of murine CYP2B10 and CYP2F2 mRNAs were significantly lower ( $p < 0.05$ ) in the dissected adjacent lung tissues from tumor-bearing mice, than in lungs from saline treated control mice (Supplemental Fig. 1A, 1B). In contrast, the levels of hepatic CYP2B10 and CYP3A11 mRNAs in the tumor-bearing mice were similar to those in the control group (Supplemental Fig. 1C, 1D). These results suggest that the lung tumorigenesis had a general, but tissue-specific effect on lung P450 expression.

### **Tumor-related inflammatory response in the NNK-treated, tumor-bearing mice**

To evaluate whether systemic inflammation was induced in the tumor-bearing mice, we measured serum levels of three proinflammatory cytokines, IL-6, TNF- $\alpha$  and IFN- $\gamma$ , by ELISA,

DMD #63305

as well as mouse hepatic SAP mRNA levels [known to respond to induction by pro-inflammatory cytokines; (Sunman et al., 2004)] by RNA-PCR. We have recently reported the large effects of systemic inflammation, induced by LPS injection, on serum levels of IL-6 and hepatic levels of SAP in the CYP2A13-humanized mouse (Wu et al., 2013). However, none of the three proinflammatory cytokines was detected in the sera of either saline-treated or NNK-treated/tumor-bearing CYP2A13-humanized mice (data not shown; detection limits were: TNF- $\alpha$  and IFN- $\gamma$ , ~30 pg/ml, IL-6, ~15 pg/ml); whereas hepatic SAP mRNA levels were very low and not significantly different between the control and tumor-bearing groups (Fig. 2A). These results indicated absence of a systemic inflammation in the tumor-bearing mice, at the time when tumors were counted (16 weeks after NNK treatment). In contrast, all three cytokines were detected, albeit at relatively low levels, in lung tissue homogenates and their levels were significantly higher ( $p < 0.05$ ) in tumor-bearing mice than in control mice (Fig. 2B-2D). These data suggest occurrence of a low grade of lung inflammation in the tumor-bearing mice that were treated with NNK at 30 or 50 mg/kg for tumor induction. In other studies not presented, more severe lung inflammation was observed in tumor-bearing mice from the 200 mg/kg-NNK group, including tissue injury and mononuclear cell infiltration.

## DISCUSSION

We found no evidence of systemic inflammation in our mouse lung tumor model, at the time when tissues were collected for analysis of CYP2A13 expression. This finding was not surprising, as systemic inflammation usually occurs only in cases of advanced cancer (Martin et al., 1999). On the other hand, local inflammation in the lungs of the tumor-bearing mice was evident, as shown by significant elevation in levels of IL-6, TNF- $\alpha$ , and IFN- $\gamma$  in lung homogenates. Thus, it is highly likely that the suppression of CYP2A13 expression observed in the present lung tumor model was mediated through tumor-derived local inflammation in the lung. In that regard, we have already shown that systemic inflammation, induced by LPS treatment, can suppress lung CYP2A13 expression in the same CYP2A13-humanized mouse model (Wu et al., 2013). Additionally, data in Figure 1D confirmed that a single-dose NNK injection per se would not repress CYP2A13 expression, prior to lung tumorigenesis.

The absence of systemic inflammation in our lung tumor model also explains the tissue specific suppression of CYP repression in the lung, but not in the liver, of NNK-treated, tumor-bearing mice. Our results contrast with a previous report that tumor-bearing mice had reduced hepatic CYP levels and altered CYP enzyme activity. By using an explant sarcoma in a transgenic mouse model of human CYP3A4 regulation, Charles and co-workers (Charles et al., 2006) demonstrated an association between the reduction in CYP3A4 expression and occurrence of tumor-derived inflammation. However, in the xenograft model of solid tumors used, the tumor mass reached ~3 g or 10% of total body weight over 17 - 21 days and acute-phase response was induced in the tumor-bearing mice. In contrast, the tumor-bearing mice in our study had normal weight gain (at the two doses examined) and the volume of tumor lesion was very small, which explains the lack of a systemic inflammation.

DMD #63305

In this study, the dissected “tumor-free” lung tissues might have contained some additional tumors that were too small to be seen. Given that CYP2A13 is normally not expressed in human lung cancer cell lines (Ling et al., 2007), we suspect that CYP2A13 expression within the tumor cells was also suppressed. This reduction would contribute to the overall decrease in CYP2A13 levels detected in the dissected “tumor-free” lung tissues from the tumor-bearing mice. Nonetheless, we estimated that the total number of tumor cells in the dissected lungs of NNK-treated mice was on average only no more than 6% of the total cells, an abundance that would not explain the more than 50% decreases in overall CYP2A13 expression level that was actually observed. Thus, we conclude that the observed decreases in CYP2A13 levels in the lungs of NNK-treated, tumor-bearing mice mainly reflect suppression of CYP2A13 expression in adjacent, histologically normal lung tissues, rather than a possible loss of CYP2A13 expression in the tumor itself.

In summary, by studying a CYP2A13-humanized mouse model, we have demonstrated for the first time that the expression of human CYP2A13 transgene was repressed in the presence of lung tumors. Accompanying the decrease in CYP2A13 expression, three proinflammatory cytokines (IL-6, TNF- $\alpha$ , and IFN- $\gamma$ ) were up-regulated in the lungs of tumor-bearing mice. These findings further support our hypothesis (Wu et al., 2013) that the low expression of CYP2A13 observed in the resected, histologically normal lung biopsy tissues from patients with lung cancers (Zhang et al., 2007) was caused at least in part by the tumor-induced chronic inflammation in the lung. In that regard, most studies on gene expression in human lungs use tissue samples that were available from patients suffering from lung diseases or from organ donors who had been subjected to surgical conditions that could induce lung inflammation. The results of these studies are commonly taken to represent tissue levels of gene expression in people (healthy or not). However, our findings imply that, for CYP2A13, the detected levels in

DMD #63305

available human lung tissue samples are much lower than the levels in healthy, intact human lungs.

DMD #63305

### **Acknowledgements**

We thank Ms. Weizhu Yang for help with mouse breeding. We gratefully acknowledge the use of the Biochemistry, Histopathology, and Advanced Light Microscopy and Image Analysis Core Facilities of the Wadsworth Center.

### **Authorship Contributions**

*Participated in research design:* Liu, Li, and Ding

*Conducted experiments:* Liu, Megaraj, Li, Sell, and Hu

*Performed data analysis:* Liu, Megaraj, Li, Sell, Hu, and Ding

*Wrote or contributed to the writing of the manuscript:* Liu, Li, and Ding

## References

- Braeuning A, Sanna R, Huelsken J, and Schwarz M (2009) Inducibility of drug-metabolizing enzymes by xenobiotics in mice with liver-specific knockout of Ctnnb1. *Drug Metab Dispos* **37**:1138-1145.
- Charles KA, Rivory LP, Brown SL, Liddle C, Clarke SJ, and Robertson GR (2006) Transcriptional repression of hepatic cytochrome P450 3A4 gene in the presence of cancer. *Clin Cancer Res* **12**:7492-7497.
- D'Agostino J, Zhang X, Wu H, Ling G, Wang S, Zhang QY, Liu F, and Ding X (2008) Characterization of CYP2A13\*2, a variant cytochrome P450 allele previously found to be associated with decreased incidences of lung adenocarcinoma in smokers. *Drug Metab Dispos* **36**:2316-2323.
- Ding X and Coon MJ (1990) Immunochemical characterization of multiple forms of cytochrome P-450 in rabbit nasal microsomes and evidence for tissue-specific expression of P-450s NMa and NMb. *Mol Pharmacol* **37**:489-496.
- Gu J, Zhang QY, Genter MB, Lipinkas TW, Negishi M, Nebert DW, and Ding X (1998) Purification and characterization of heterologously expressed mouse CYP2A5 and CYP2G1: role in metabolic activation of acetaminophen and 2,6-dichlorobenzonitrile in mouse olfactory mucosal microsomes. *J Pharmacol Exp Ther* **285**:1287-1295.
- He XY, Shen J, Ding X, Lu AY, and Hong JY (2004) Identification of critical amino acid residues of human CYP2A13 for the metabolic activation of 4-(methylnitrosamino)-1-(3-pyridyl)-1-butanone, a tobacco-specific carcinogen. *Drug Metab Dispos* **32**:1516-1521.
- Jalas JR, Hecht SS, and Murphy SE (2005) Cytochrome P450 enzymes as catalysts of metabolism of 4-(methylnitrosamino)-1-(3-pyridyl)-1-butanone, a tobacco specific carcinogen. *Chem Res Toxicol* **18**:95-110.
- Koskela S, Hakkola J, Hukkanen J, Pelkonen O, Sorri M, Saranen A, Anttila S, Fernandez-Salguero P, Gonzalez F, and Raunio H (1999) Expression of CYP2A genes in human liver and extrahepatic tissues. *Biochem Pharmacol* **57**:1407-1413.
- Ling G, Wei Y, and Ding X (2007) Transcriptional regulation of human CYP2A13 expression in the respiratory tract by CCAAT/enhancer binding protein and epigenetic modulation. *Mol Pharmacol* **71**:807-816.
- Martin F, Santolaria F, Batista N, Milena A, Gonzalez-Reimers E, Brito MJ, and Oramas J (1999) Cytokine levels (IL-6 and IFN-gamma), acute phase response and nutritional status as prognostic factors in lung cancer. *Cytokine* **11**:80-86.
- Megaraj V, Zhou X, Xie F, Liu Z, Yang W, and Ding X (2014) Role of CYP2A13 in the bioactivation and lung tumorigenicity of the tobacco-specific lung procarcinogen 4-(methylnitrosamino)-1-(3-pyridyl)-1-butanone: in vivo studies using a CYP2A13-humanized mouse model. *Carcinogenesis* **35**:131-137.
- Pan J, Xiang Q, and Ball S (2000) Use of a novel real-time quantitative reverse transcription-polymerase chain reaction method to study the effects of cytokines on cytochrome P450 mRNA expression in mouse liver. *Drug Metab Dispos* **28**:709-713.
- Su T, Bao Z, Zhang QY, Smith TJ, Hong JY, and Ding X (2000) Human cytochrome P450 CYP2A13: predominant expression in the respiratory tract and its high efficiency metabolic activation of a tobacco-specific carcinogen, 4-(methylnitrosamino)-1-(3-pyridyl)-1-butanone. *Cancer Res* **60**:5074-5079.
- Sunman JA, Hawke RL, LeCluyse EL, and Kashuba AD (2004) Kupffer cell-mediated IL-2 suppression of CYP3A activity in human hepatocytes. *Drug Metab Dispos* **32**:359-363.



DMD #63305

- Wang H, Tan W, Hao B, Miao X, Zhou G, He F, and Lin D (2003) Substantial reduction in risk of lung adenocarcinoma associated with genetic polymorphism in CYP2A13, the most active cytochrome P450 for the metabolic activation of tobacco-specific carcinogen NNK. *Cancer Res* **63**:8057-8061.
- Wei Y, Li L, Zhou X, Zhang QY, Dunbar A, Liu F, Kluetzman K, Yang W, and Ding X (2013) Generation and characterization of a novel Cyp2a(4/5)bgs-null mouse model. *Drug Metab Dispos* **41**:132-140.
- Wei Y, Wu H, Li L, Liu Z, Zhou X, Zhang QY, Weng Y, D'Agostino J, Ling G, Zhang X, Kluetzman K, Yao Y, and Ding X (2012) Generation and characterization of a CYP2A13/2B6/2F1-transgenic mouse model. *Drug Metab Dispos* **40**:1144-1150.
- Wong HL, Zhang X, Zhang QY, Gu J, Ding X, Hecht SS, and Murphy SE (2005) Metabolic activation of the tobacco carcinogen 4-(methylnitrosamino)-(3-pyridyl)-1-butanone by cytochrome P450 2A13 in human fetal nasal microsomes. *Chem Res Toxicol* **18**:913-918.
- Wu H, Liu Z, Ling G, Lawrence D, and Ding X (2013) Transcriptional suppression of CYP2A13 expression by lipopolysaccharide in cultured human lung cells and the lungs of a CYP2A13-humanized mouse model. *Toxicol Sci* **135**:476-485.
- Wu H, Zhang X, Ling G, D'Agostino J, and Ding X (2009) Mechanisms of differential expression of the CYP2A13 7520C and 7520G alleles in human lung: allelic expression analysis for CYP2A13 heterogeneous nuclear RNA, and evidence for the involvement of multiple cis-regulatory single nucleotide polymorphisms. *Pharmacogenet Genomics* **19**:852-863.
- Zhang X, Caggana M, Cutler TL, and Ding X (2004) Development of a real-time polymerase chain reaction-based method for the measurement of relative allelic expression and identification of CYP2A13 alleles with decreased expression in human lung. *J Pharmacol Exp Ther* **311**:373-381.
- Zhang X, D'Agostino J, Wu H, Zhang QY, von Weymarn L, Murphy SE, and Ding X (2007) CYP2A13: variable expression and role in human lung microsomal metabolic activation of the tobacco-specific carcinogen 4-(methylnitrosamino)-1-(3-pyridyl)-1-butanone. *J Pharmacol Exp Ther* **323**:570-578.
- Zhang X, Su T, Zhang QY, Gu J, Caggana M, Li H, and Ding X (2002) Genetic polymorphisms of the human CYP2A13 gene: identification of single-nucleotide polymorphisms and functional characterization of an Arg257Cys variant. *J Pharmacol Exp Ther* **302**:416-423.
- Zhu LR, Thomas PE, Lu G, Reuhl KR, Yang GY, Wang LD, Wang SL, Yang CS, He XY, and Hong JY (2006) CYP2A13 in human respiratory tissues and lung cancers: an immunohistochemical study with a new peptide-specific antibody. *Drug Metab Dispos* **34**:1672-1676.

DMD #63305

### **Footnotes**

This work was supported in part by the National Institutes of Health [Grant CA092596].

### **ADDRESS CORRESPONDENCE TO:**

Dr. Xinxin Ding, College of Nanoscale Science and Engineering, SUNY Polytechnic Institute,  
257 Fuller Road, NanoFab East, Albany, NY 12203; Tel. 518-956-7057; E-mail:

[xding@sunycnse.com](mailto:xding@sunycnse.com)

DMD #63305

## Figures Legends

**Fig. 1.** Effects of lung tumorigenesis on CYP2A13 expression in adjacent lung tissues of CYP2A13-humanized mice. Mice (2-month old females) were treated with saline (control) or with NNK (either 30 or 50 mg/kg, once, i.p.), and tissues were obtained 1 or 16 weeks after dosing. Dissected lung tissues with no visible tumors were used for preparation of microsomes (from tissues pooled from 2-4 mice) or RNA (from tissues of individual mice). **A**, Immunoblot analysis of CYP2A13 expression. Microsomal protein (10  $\mu$ g/lane) was analyzed in duplicate, with use of an anti-CYP2A5 polyclonal antibody. Lung microsomes of a *Cyp2a5*-null mouse were also analyzed as a negative control. Calnexin was detected as a loading control. Representative results of three different batches of pooled microsomes are shown. **B**, Densitometry results of immunoblot analysis for three separate pools of dissected lung tissues (means  $\pm$  S.E., n=3, normalized by the level of calnexin). **C-D**, CYP2A13 mRNA levels at 16 weeks (C) or 1 week (D) after NNK treatment. The values shown represent means  $\pm$  S.E. (n=3-8), normalized by the level of murine GAPDH. \*\*\*,  $p < 0.001$ ; \*\*,  $p < 0.01$ ; compared to the saline control group; one-way ANOVA with Dunnett's post hoc test.

**Fig. 2.** Levels of SAP mRNA in the liver and proinflammatory cytokines in the lung of CYP2A13-humanized mice. **A**, SAP mRNA levels in the liver of mice treated with NNK (either 30 or 50 mg/kg, combined as one group) or saline. Tissues were obtained 16 weeks after dosing. Data represent means  $\pm$  S.E. (n=4 for saline, n=10 for NNK), normalized by the level of murine GAPDH.  $p > 0.05$ ; Student's t-test. **B-D**, Levels of IL-6, IFN- $\gamma$  and TNF- $\alpha$  in lung tissue homogenate (pg/mg total protein). Dissected lung tissues with no visible tumors (from individual mice) were used for preparation of tissue homogenate. For saline-treated/tumor-free mice, the lungs were used without dissection. Data represent means  $\pm$  S.E. (n=3 for saline, n=6 for NNK, either 30 or 50 mg/kg). \*,  $p < 0.05$ , compared to saline control group; Student's t-test.

Fig. 1

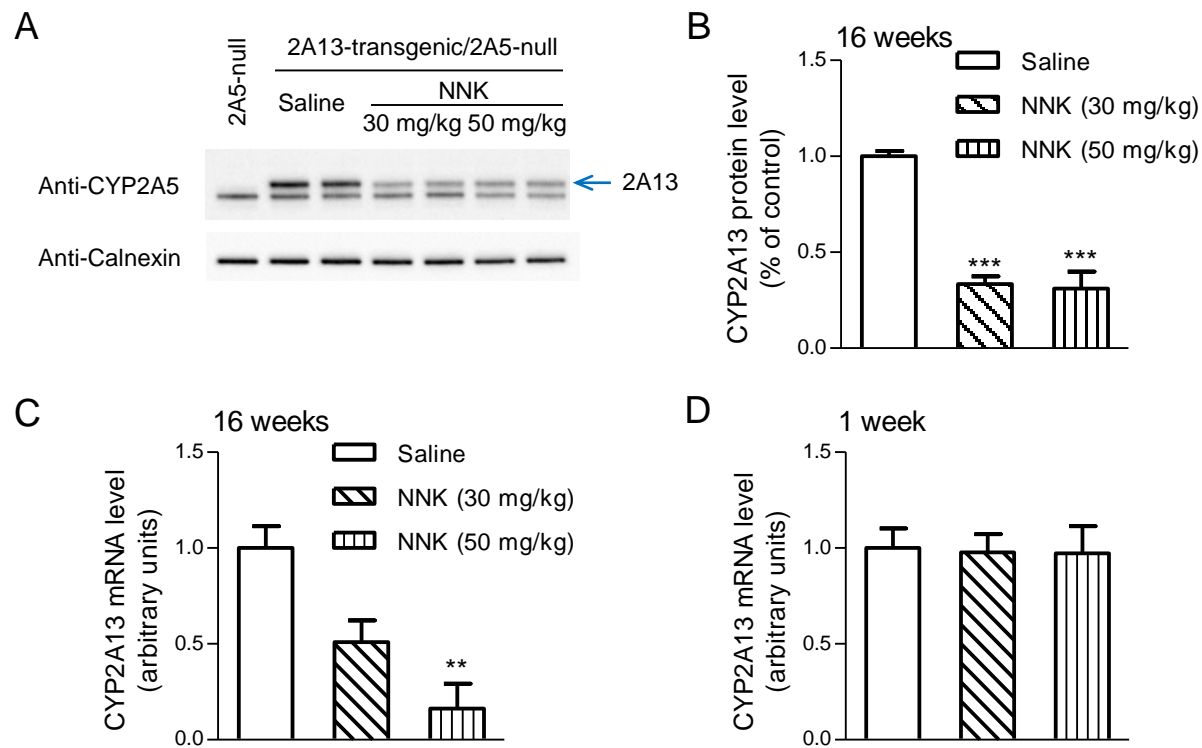


Fig. 2

